5548 *Chem. Mater.* **2009,** *21,* 5548–5555
DOI:10.1021/cm9028935

CHEMISTRY OF MATERIALS
Article

Double Emulsion Droplets as Microreactors for Synthesis of Mesoporous Hydroxyapatite

Ho Cheung Shum,[†] Amit Bandyopadhyay,[§] Susmita Bose,*[,§] and David A. Weitz*[,†,‡]

[†]*School of Engineering and Applied Sciences and,* [‡]*Department of Physics, Harvard University, Cambridge, Massachusetts 02138, and* [§]*School of Mechanical and Materials Engineering, Washington State University, Pullman, Washington 99164*

Received September 16, 2009

We introduce a novel approach for synthesizing mesoporous hydroxyapatite (HAp, $(Ca)_{10}$, $(PO_4)_6(OH)_2$) using double emulsion droplets as microreactors. By using capillary microfluidic techniques, the size and the geometry of the droplet microreactors can be tuned easily. Double emulsion droplets offer the combined advantages of both shielding the reactants and on-demand addition of reactants; this makes them highly versatile microreactors. Such droplet microreactors also enable simple visualization of the HAp formation process as well as control over the porosity in the HAp that is synthesized. Powder formed with our technique demonstrates a remarkable microstructure, as well as significantly enhanced BET specific average surface area and nanoscale porosity. Our results present a novel synthesis approach for controlling the nanoscale porosity and the morphology of inorganic particles using double emulsion droplets.

Introduction

The biocompatibility and chemical similarity to bone makes calcium phosphate (CaP) based ceramic materials, especially hydroxyapatite (HAp), a widely used material of choice for orthopedic, dental, and other biorelated applications.[1−3] To mimic the functions of their counterparts in natural biological systems, CaP-based materials are often used in conjunction with different biomolecules to provide surfaces for adsorption and catalysis of biochemical reactions.[3−5] The adsorption of biomolecules onto the surface of these CaP-based materials depends critically on their structural properties such as microstructures, surface area, and porosity.[6] For example, introduction of nanosized pores in these materials can not only significantly enhance the total surface area but also promote integration of biomolecules and drugs with the particles. Various synthesis and processing techniques have been developed for these CaP-based materials, including solid-state-reaction,[7] coprecipitation,[8,9] sol−gel,[10−16] hydrothermal,[17−19] and surfactant-templated[20−22] methods. While CaPs prepared with these techniques show improved mechanical and surface properties as well as good bioactivity, agglomeration of final powders cannot be easily controlled.[10] To control its morphology and shape, HAp nanopowder has been synthesized inside microemulsion droplets or reverse micelles, which act as microreactors separated from each other by an organic continuous phase.[23−27] However, it remains difficult to produce HAp nanopowder with very high surface

*E-mail: sbose@wsu.edu; weitz@seas.harvard.edu.

(1) Burg, K. J. L.; Porter, S.; Kellam, J. F. *Biomaterials* **2000**, *21*(23), 2347–2359.
(2) Vallet-Regí, M.; González-Calbet, J. M. *Prog. Solid State Chem.* **2004**, *32*(1−2), 1–31.
(3) El-Ghannam, A. *Exp. Rev. Med. Dev.* **2005**, *2*(1), 87–101.
(4) Oonishi, H. L. L. H. J. W. F. S. E. T. S. K. H. I. *J. Biomed. Mater. Res.* **1999**, *44*(1), 31–43.
(5) Karageorgiou, V.; Kaplan, D. *Biomaterials* **2005**, *26*(27), 5474–5491.
(6) Shane, A. C.; Marc, D. F.; Yogesh, K. V.; William, R. L.; Jack, E. L.; Shanna, W.; Ramakrishna, V. *J. Nanosci. Nanotechnol.* **2002**, *2*, 293–312.
(7) Rao, R. R.; Roopa, H. N.; Kannan, T. S. *J. Mater. Sci.-Mater. Med.* **1997**, *8*(8), 511–518.
(8) Tas, A. C.; Korkusuz, F.; Timucin, M.; Akkas, N. *J. Mater. Sci.-Mater. Med.* **1997**, *8*(2), 91–96.
(9) Sang-Hoon Rhee, J. T. *J. Am. Ceram. Soc.* **1998**, *81*(11), 3029–3031.
(10) Bose, S.; Saha, S. K. *J. Am. Ceram. Soc.* **2003**, *86*(6), 1055–1057.
(11) Pierre Layrolle, A. I. T. T. *J. Am. Ceram. Soc.* **1998**, *81*(6), 1421–1428.
(12) Jillavenkatesa, A.; Condrate, R. A. *J. Mater. Sci.* **1998**, *33*(16), 4111–4119.
(13) Eshtiagh-Hosseini, H.; Housaindokht, M. R.; Chahkandi, M. *Mater. Chem. Phys.* **2007**, *106*(2−3), 310–316.
(14) Fathi, M. H.; Hanifi, A. *Mater. Lett.* **2007**, *61*(18), 3978–3983.
(15) Bogdanoviciene, I.; Beganskiene, A.; Tonsuaadu, K.; Glaser, J.; Meyer, H. J.; Kareiva, A. *Mater. Res. Bull.* **2006**, *41*(9), 1754–1762.
(16) Liu, D. M.; Troczynski, T.; Tseng, W. J. *Biomaterials* **2001**, *22*(13), 1721–1730.
(17) Liu, H. S.; Chin, T. S.; Lai, L. S.; Chiu, S. Y.; Chung, K. H.; Chang, C. S.; Lui, M. T. *Ceram. Int.* **1997**, *23*, 19–25.
(18) Kothapalli, C. R.; Wei, M.; Legeros, R. Z.; Shaw, M. T. *J. Mater. Sci.: Mater. Med.* **2005**, *16*, 441−446.
(19) Liu, R. F.; Xiao, X. F.; Ni, J.; Huang, J. M. *Chin. J. Inorg. Chem.* **2003**, *19*(10), 1079–1084.
(20) Wu, Y. J.; Bose, S. *Langmuir* **2005**, *21*(8), 3232–3234.
(21) Ikawa, N.; Hori, H.; Kimura, T.; Oumi, Y.; Sano, T. *Langmuir* **2008**, *24*, 13113–13120.
(22) Yuan, Z. Y.; Liu, J. Q.; Peng, L. M.; Su, B. L. *Langmuir* **2002**, *18*(6), 2450–2452.
(23) Norton, J.; Malik, K. R.; Darr, J. A.; Rehman, I. *Adv. Appl. Ceram.* **2006**, *105*, 113–139.
(24) Sadasivan, S.; Khushalani, D.; Mann, S. *Chem. Mater.* **2005**, *17* (10), 2765–2770.
(25) Koumoulidis, G. C.; Katsoulidis, A. P.; Ladavos, A. K.; Pomonis, P. J.; Trapalis, C. C.; Sdoukos, A. T.; Vaimakis, T. C. *J. Colloid Interface Sci.* **2003**, *259*(2), 254–260.
(26) Banerjee, A.; Bandyopadhyay, A.; Bose, S. *Mater. Sci. Eng. C−Biomim. Supramolec. Syst.* **2007**, *27*(4), 729–735.
(27) Bose, S.; Saha, S. K. *Chem. Mater.* **2003**, *15*(23), 4464–4469.

 Published on Web 10/16/2009

area, as determined by the Brunauer−Emmett−Teller (BET) techniques; this is advantageous for both densification as well as bone morphogenic protein or drug delivery applications when synthetic CaPs are used in treatments for bone related disorders. More importantly, most conventional methods involve intermediate processing steps that prevent in situ visualization of formation of the inorganic nanoparticles. As a result, the exact mechanism for the formation of CaPs from its precursor materials is still not well understood.

A novel strategy to fabricate HAp nanopowder is to utilize droplets as reactors, each of which can be monitored individually. The homogeneity of the final powders is governed by the uniformity of the droplets. By flowing fluids through microchannels of hundreds of micrometers in size, microfluidic emulsification offers a means to prepare emulsions with a narrow size distribution by providing a high degree of control over the emulsion generation process.[28,29] The resulting single emulsion droplets have been demonstrated to be ideal templates for fabricating monodisperse particles, highlighting the versatility and controllability of the technique.[30−34] Moreover, due to relatively larger droplet size compared with conventional emulsion techniques, subsequent processing of the droplets can be easily monitored with microscopy techniques. The high degree of control afforded by the microfluidic apparatus makes it possible to prepare not only single emulsion droplets, but also multiple emulsions.[28,29,35] For instance, water-in-oil-in-water (W/O/W) double emulsions have been used as templates for assembling amphiphiles to form vesicles with high size uniformity and with high encapsulation efficiency.[36,37] While controlled W/O/W double emulsion droplets have been used as templates for fabricating core−shell structures such as colloidosomes[38] and gel shells,[39] their use as microreactors has not been extensively explored. Double emulsion droplets are advantageous as microreactors because droplets are prevented from agglomerating with neighboring droplets by the middle oil shell surrounding the reacting core. Additional reactants can also be added to the microreactors by diffusion through the middle oil shells. The abilities to segregate reacting droplets from each other and also to allow additional reactants to be added to the droplets highlight the versatility of double emulsion droplets as microreactors.

In the present work, we synthesize HAp using double emulsion droplets as microreactors. A glass capillary microfluidic setup is used for generating double emulsion microreactors with calcium and phosphorus precursors encapsulated in the inner aqueous droplets. Formation of HAp is triggered by adding an alkali to the continuous phase to adjust the pH. Since the alkaline solution is miscible with the continuous phase, no additional homogenization treatment is required. Powders obtained with this technique are shown to exhibit unique microstructures with very high surface area and mesoporosity. The double-emulsion-droplet technique represents a novel approach for synthesis of inorganic powders and offers a means to understand the formation mechanism through direct visualization. The technique also opens up a new synthesis approach for inorganic powder particles in which the morphology and the nanoscale porosity can be controlled.

Materials and Methods

Water-in-oil-in-water (W/O/W) double emulsion drops were produced using glass microcapillary devices. The inner phase consisted of 0.1−1 M calcium nitrate tetrahydrate ($Ca(NO_3)_2 \cdot 4H_2O$, ≥99.0%, SigmaUltra, St. Louis, MO) and 0.071−0.71 M phosphoric acid (H_3PO_4, orthophosphoric acid, ≥85%, Fluka, St. Louis, MO) in water. The osmolality of the solutions was measured with a micro-osmometer (Advanced Instruments, Inc., model 3300). Unless otherwise noted, the middle oil phase consisted of 2 wt % surfactant (Dow Corning 749 fluid, Midland, MI) in a silicone oil (Dow Corning 200 Fluid, 5 cSt, Midland, MI). The outer phase was a 5 wt % poly vinyl alcohol aqueous solution (PVA; M_w 13 000−23 000 $g \cdot mol^{-1}$, 87−89% hydrolyzed, Aldrich, St. Louis, MO). The surfactant stabilized the inner drops against coalescence with the exterior aqueous phase, while PVA prevented coalescence of the oil drops. The pH of the double emulsion formed was adjusted by adding 0.1 N ammonium hydroxide solution (NH_4OH, Fluka, St. Louis, MO) to the continuous phase. The outer phase was prepared in some runs by dissolving PVA directly in 0.1 N NH_4OH solution to achieve a one-step synthesis of HAp particle aggregatates. A schematic of the process is shown in Figure 1. Unless otherwise specified, all other chemicals were obtained from Aldrich. Water with a resistivity of 18.2 $M\Omega\ cm^{-1}$ was acquired from a Millipore Milli-Q system (Millipore, Billerica, MA).

Preparation of Double Emulsions. Monodisperse W/O/W double emulsions were prepared using glass microcapillary devices, as shown schematically in Figure 2a.[29] The round capillaries (World Precision Instruments, Inc., Sarasota, FL), with inner and outer diameters of 0.58 and 1.0 mm, respectively, were tapered to desired diameters with a micropipet puller (P-97, Sutter Instrument, Inc.) and a microforge (Narishige International USA, Inc., East Meadow, NY). Two tapered capillaries were aligned inside square glass capillaries (Altantic International Technology, Inc., Rockaway, NJ) with an inner dimension of 1.05 mm. A transparent epoxy resin (5 minute Epoxy,

(28) Shah, R. K.; Shum, H. C.; Rowat, A. C.; Lee, D.; Agresti, J. J.; Utada, A. S.; Chu, L. Y.; Kim, J. W.; Fernandez-Nieves, A.; Martinez, C. J.; Weitz, D. A. *Mater. Today* **2008**, *11*(4), 18–27.
(29) Utada, A. S.; Lorenceau, E.; Link, D. R.; Kaplan, P. D.; Stone, H. A.; Weitz, D. A. *Science* **2005**, *308*(5721), 537–541.
(30) Dubinsky, S.; Zhang, H.; Nie, Z. H.; Gourevich, I.; Voicu, D.; Deetz, M.; Kumacheva, E. *Macromolecules* **2008**, *41*(10), 3555–3561.
(31) Engl, W.; Backov, R.; Panizza, P. *Curr. Opin. Colloid Interface Sci.* **2008**, *13*(4), 206–216.
(32) Serra, C. A.; Chang, Z. Q. *Chem. Eng. Technol.* **2008**, *31*(8), 1099–1115.
(33) Xu, J. H.; Li, S. W.; Tan, J.; Luo, G. S. *Chem. Eng. Technol.* **2008**, *31*(8), 1223–1226.
(34) Xu, S. Q.; Nie, Z. H.; Seo, M.; Lewis, P.; Kumacheva, E.; Stone, H. A.; Garstecki, P.; Weibel, D. B.; Gitlin, I.; Whitesides, G. M. *Angew. Chem., Int. Ed.* **2005**, *44*(5), 724–728.
(35) Chu, L. Y.; Utada, A. S.; Shah, R. K.; Kim, J. W.; Weitz, D. A. *Angew. Chem., Int. Ed.* **2007**, *46*(47), 8970–8974.
(36) Shum, H. C.; Kim, J. W.; Weitz, D. A. *J. Am. Chem. Soc.* **2008**, *130* (29), 9543–9549.
(37) Shum, H. C.; Lee, D.; Yoon, I.; Kodger, T.; Weitz, D. A. *Langmuir* **2008**, *24*(15), 7651–7653.
(38) Lee, D.; Weitz, D. A. *Adv. Mater.* **2008**, *20*(18), 3498–3503.
(39) Kim, J. W.; Utada, A. S.; Fernandez-Nieves, A.; Hu, Z. B.; Weitz, D. A. *Angew. Chem., Int. Ed.* **2007**, *46*(11), 1819–1822.

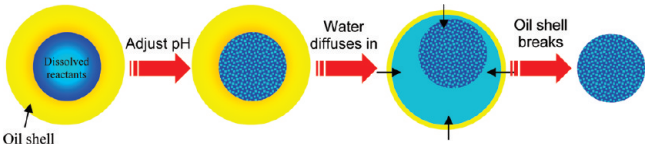

Figure 1. Schematic illustration of the double-emulsion-templated synthesis of hydroxyapatite. The inner drops of the double emulsion consist of an aqueous solution of calcium nitrate and phosphoric acid, which are the calcium and the phosphorus precursors. The oil shells surrounding the inner drops are made up of an inert oil phase. Upon increase of pH by adding ammonium hydroxide to the continuous phase, hydroxyapatite is formed in the inner drops of the emulsion. Due to their higher osmolality, water diffuses into and swells the inner drops, leading to an increase in size of the double emulsion drops and a resulting thinning of the oil shells. Eventually, the oil shells become so thin that the double emulsions destabilize, releasing the hydroxyapatite cores.

Devcon, Danvers, MA) was applied to seal the capillaries where necessary. The outer radii, R_o, of the double emulsions ranged from 40 to 80 μm, while the inner radii, R_i, ranged from 30 to 70 μm. These values were controlled by the size of the capillaries and the flow rates of the different phases.[29] The calcium and phosphorus precursors were predissolved in the inner phase for subsequent encapsulation in double emulsion drops. Positive syringe pumps (PHD 2000 series, Harvard Apparatus, Holliston, MA) were used to deliver the different phases at desired flow rates. A typical set of flow rates for the outer, middle, and inner phases was 10, 2.2, and 1.2 mL/h, respectively, and the droplet-generation frequency was about 1000 Hz. Samples were collected between a coverslip and a glass slide separated by a 0.5-mm-thick silicone isolator. The isolator was prefilled with 0.1 N ammonium hydroxide solution for pH adjustment. The subsequent formation of HAp was monitored with optical microscopy.

Preparation of Hydroxyapatite (HAp) Powders. To prepare HAp powders, double emulsions with calcium and phosphorus precursors in the inner drops were collected in vials of 0.1 N ammonium hydroxide solution; this triggers the formation of hydroxyapaptite. After the vials were completely filled, they were capped and sealed with parafilm. The vials were then left tumbling on a tumbler, during which water continuously diffused from the continuous phase to the inner drops due to an osmotic pressure difference. The double emulsion drops eventually destabilized, releasing the as-formed HAp powders. To wash these HAp powders, the remaining oil phase in the vials was removed and the aqueous supernatant was replaced with fresh water. After repeating the washing step for 5 times, the remaining HAp was dried in an oven at 40 °C for 3−7 days to obtain a dry powder for further characterization. The dry powder was characterized both before and after calcination at elevated temperatures.

Direct Visualization of HAp Formation in Double Emulsions. Optical-microscopy images were obtained with 10×, 40×, and 63× objectives at room temperature using an inverted microscope (DMIRBE, Leica, Wetzlar, Germany), an inverted fluorescence microscope (DMIRB, Leica, Wetzlar, Germany), or an upright fluorescence microscope (DMRX, Leica, Wetzlar, Germany) equipped with a high speed camera (Phantom, V5, V7 or V9, Vision Research, Wayne, NJ) or a digital camera (QICAM 12-bit, Qimaging, Surrey, British Columbia, Canada). All double-emulsion-generation processes were monitored with the microscope using a high-speed camera. The formation mechanism of HAp from double emulsions and the resulting HAp powders were imaged using a digital camera.

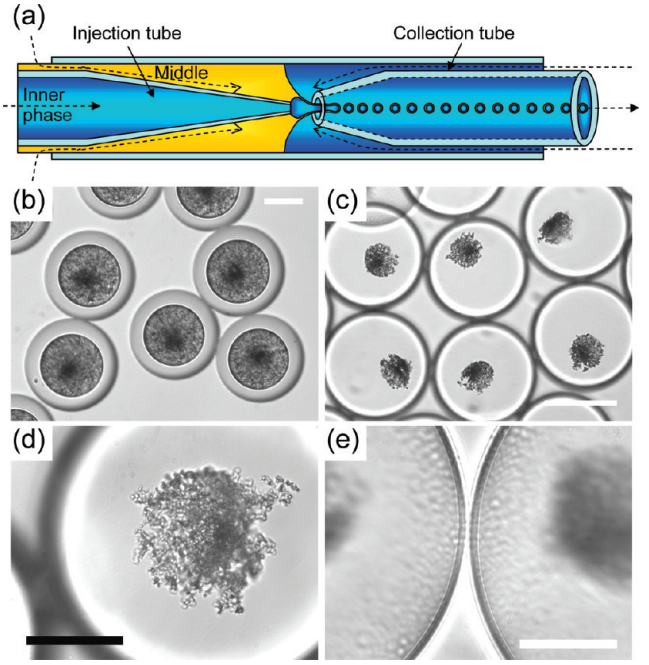

Figure 2. (a) Schematic of the glass microcapillary device for generating double emulsion droplets. (b−e) Optical microscope images of double emulsion drops (b) immediately and (c) 91 h after addition of 0.1 N ammonium hydroxide solution. The change in pH triggers the formation of hydroxyapatite in the inner drops of the double emulsion. The hydroxyapatite initially spans the entire volume of the inner drops. As water diffuses into the inner drops due to a higher internal osmolality, the hydroxyapatite aggregates remain roughly the same in size. Optical microscope images of (d) a hydroxyapatite particle aggregate formed and (e) oil shells at higher magnification. The thickness of the oil shells has reduced from 18 to 4.8 μm after 91 h. Scale bars are 50 μm for parts b, d, and e and 150 μm for part c.

Characterization of HAp Powders. *Microstructural Analysis.* Scanning electron microscopic (SEM) images of dried powders were taken using a Zeiss Supra 55 VP field emission scanning electron microscope (FESEM, Carl Zeiss, Germany) at an acceleration voltage of 20 kV. Transmission electron microscope (TEM) images were taken on a JEOL JEM-2010 TEM (JEOL, Tokyo, Japan) operated at 200 kV. TEM samples were prepared using a drop of suspension with high volume fraction of as-formed HAp on a 200 or 300 mesh copper grid coated with Lacey carbon (Electron Microscopy Sciences, Hatfield, PA).

BET Specific Average Surface Area Analysis. Adsorption and desorption measurements were performed using a Beckman Coulter SA 3100 surface area and pore size analyzer (Beckman Coulter, Fullerton, CA) with nitrogen as an adsorbate. The Brunauer−Emmett−Teller (BET) surface areas were calculated from $p/p_0 = 0.3$ in the adsorption curve using the BET equation.[40] The pore size distributions were calculated from the desorption and the adsorption data using the Barrett−Joyner−Halenda (BJH) model.[41] Prior to each sorption measurement, the sample was outgassed for 1 h at 300 °C under vacuum.

Phase Analysis. Thermogravemetric analysis (TGA, Q50, TA Instruments, New Castle, DE) was performed to determine the phase transformation temperatures for the as-formed powder.

(40) Brunauer, S.; Emmett, P. H.; Teller, E. *J. Am. Chem. Soc.* **1938**, *60* (2), 309–319.
(41) Barrett, E. P.; Joyner, L. G.; Halenda, P. P. *J. Am. Chem. Soc.* **1951**, *73*(1), 373–380.

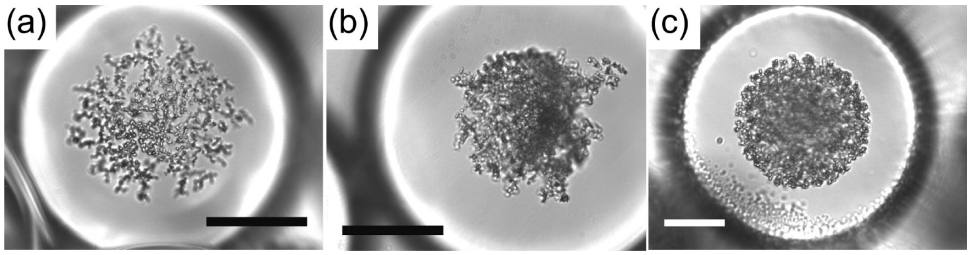

Figure 3. Optical microscope images of hydroxyapatite aggregates formed from precursor solutions with calcium nitrate and phosphoric acid concentrations of (a) 0.1 and 0.06 M, (b) 0.5 and 0.3 M, and (c) 1 and 0.6 M, respectively. The structure of the aggregates formed becomes more compact as the precursor concentration increases. Scale bars are 50 μm for parts a and b and 30 μm for part c.

Phase analysis of the powders before and after calcinations were performed by powder X-ray diffraction (XRD) using a Scintag XDS2000 fixed sample position powder diffractometer (Scintag, Cupertino, CA) with Cu Kα radiation at 40 kV and 30 mA. The XRD patterns were taken at room temperature in the range of $12° \leq 2\theta \leq 70°$ with a scan rate of 1°/min and a step size of 0.02°.

Results and Discussion

Synthesis of Mesoporous HAp in Double Emulsions. Monodisperse W/O/W double emulsions droplets are used as reactors where calcium nitrate and phosphoric acid are stored in the inner droplets for the synthesis of HAp. The synthesis is initiated after the addition of ammonium hydroxide according to the following equation:

$$10\ Ca(NO_3)_2 \cdot 4H_2O + 6\ H_3PO_4 + 20\ NH_4OH$$
$$Ca_{10}(PO_4)_6(OH)_2 + 20\ NH_4NO_3 + 22\ H_2O$$

By adjusting the reactant concentration such that the osmotic pressure is always higher in the inner drop than in the continuous phase, water can continuously diffuse into the inner drops. This leads to swelling of the inner drops and a reduction in the thickness of the oil shells. The HAp formed inside the inner drop is eventually released after the oil shells become too thin to stabilize the double emulsion, as shown schematically in Figure 1.

The reaction is completed immediately after pH adjustment by adding ammonium hydroxide, as suggested by the instantaneous precipitation shown in Figure 2b. The increase of pH in the inner droplets is made possible by the addition of ammonium hydroxide, which does not dissociate completely in water. Therefore, the undissociated ammonia molecules can diffuse across the hydrophobic oil shell. The originally transparent inner droplets become turbid as soon as the droplets come into contact with the alkaline solution. No precipitation is observed outside the inner droplets indicating that the time scale for the diffusion of the reactants through the oil shells is larger than that for the pH adjustment and precipitation reaction. The behavior is uniform for all observable droplets. Unlike typical reaction vessels, such as round-bottom flasks and test tubes, the reactants are not all mixed together; instead, reactants that can permeate the shell of the double emulsion by diffusion, are added in a subsequent step to trigger the reaction.

The size uniformity of the droplet microreactors enables visualization of multiple precipitation reactions simultaneously. Due to high concentration of the reactants in the inner drops, the osmolality is typically much higher in the inner drop. An inner solution with calcium and phosphorus precursor concentrations of 0.5 and 0.3 M, respectively, has an osmolality of ~1600 mOsm compared to ~100 mOsm for the outer continuous phase. The resulting osmotic pressure difference causes water to diffuse from the continuous phase to the inner drops, leading to their swelling. The large osmotic pressure difference may also contribute to the slow diffusion of reactants out of the inner drops and the fast pH adjustment in the inner drop due to the addition of ammonium hydroxide in the continuous phase. The solid precipitated structures remain compact without any change in size after swelling, as shown in Figure 2c. The parts of the precipitates that were bound by the oil−water interface are now freely suspended in the inner aqueous phase, as shown in Figure 2d. Since the volume of the oil shells, V_{shell}, surrounding the inner drops remains constant, the thickness of the oil shell, l, decreases with the increase in radius of the inner drop, R, as $l = V_{shell}/4\pi R^2$ for small shell thickness. The thickness of the oil shell in Figure 2e decreased from 18 to 4.8 μm after 91 h. As the shell gets thinner, it becomes more likely for the double emulsion droplets to destabilize, releasing the precipitates.

The versatility of the technique can be illustrated by the ease in tuning the micro- and nanoscale porosity of the precipitate structures; these can be adjusted by changing the concentrations of calcium and phosphorus precursors. The precipitate aggregate has an open porous structure when an inner solution with calcium and phosphorus precursor concentrations of 0.1 and 0.06 M are used, as shown in Figure 3a. All the individual precipitate particles that form the overall aggregate and their attachment points to one another can be clearly seen. As the calcium precursor concentration is increased to 0.5 M while maintaining the same calcium to phosphorus ratio, the aggregate formed has a denser structure, as shown in Figure 3b. Individual particles cannot be distinguished anymore except for those near the edge of the precipitate, where the particles span outward into the solution. As the precursor concentrations are increased further to 1 and 0.6 M for calcium and phosphorus, respectively, the aggregate structure becomes highly dense with the lowest level of porosity. On the basis of these results, we believe

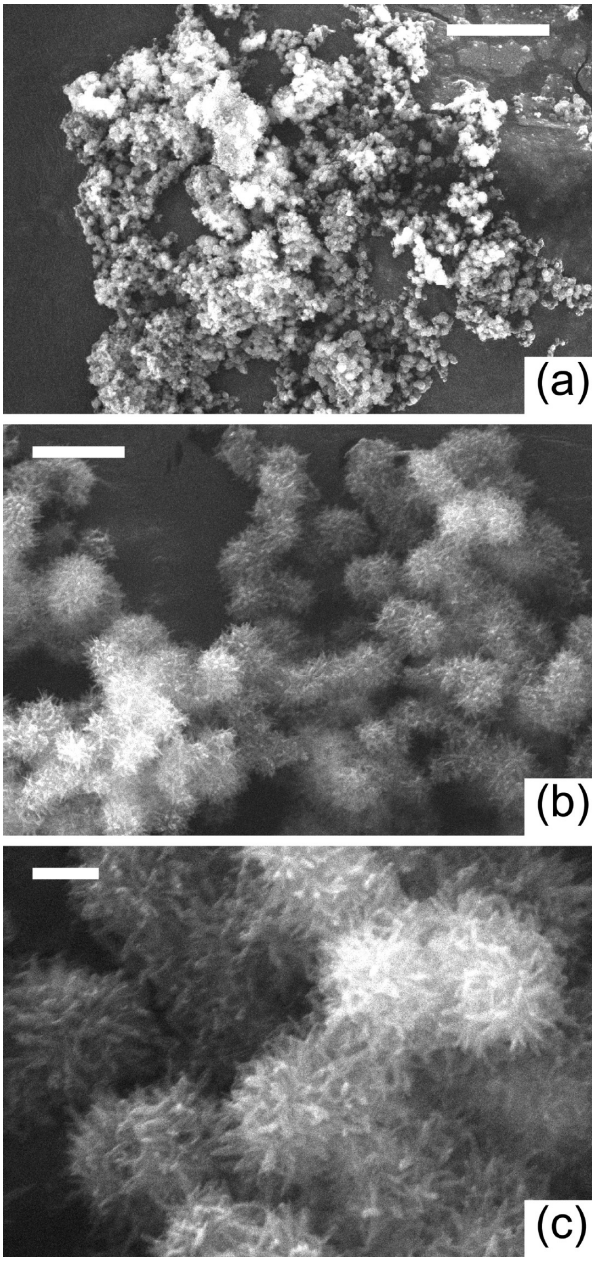

Figure 4. (a−c) Scanning electron microscope (SEM) images of dried hydroxyapatite powder at different magnifications. The hydroxyapatite formed is made up of smaller spherical particles of about 1 μm in size, as shown in part b. Each spherical particle has an open, feathery morphology shown in part c. The powder in the images was formed from a precursor solution of 0.5 M calcium nitrate and 0.3 M phosphoric acid. Scale bars are 20 μm for part a, 2 μm for part b, and 500 nm for part c.

that the precipitates form when ammonium hydroxide diffuses into the inner droplets. These precipitates then stick with each other to form a larger aggregate. If the starting reactant concentration is low, the collisions that lead to the aggregation are diffusion-limited, leading to the more open structures, as shown in Figure 3a. By contrast, with a sufficiently high reactant concentration, diffusion-induced collisions are less important in the formation of the aggregates and a more dense aggregate structure results, as shown in Figure 3b. Apart from the porosity, the size of the precipitate formed can also be easily adjusted, by varying the size of the double emulsion

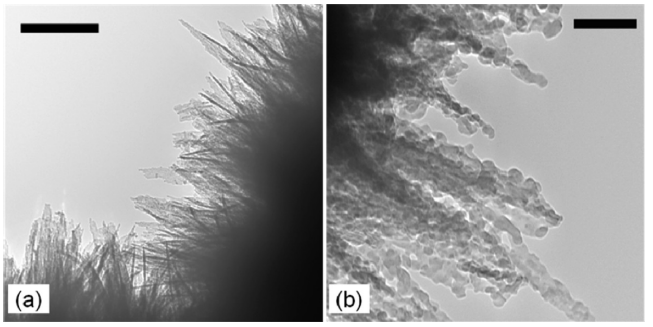

Figure 5. (a) Transmission electron microscope (TEM) image of hydroxyapatite powder. (b) Magnified view of the hairs similar to the ones shown in part a. The microstructure of the powder is dominated by nanometer-scaled needlelike nanoparticles shown in part b. The powder in the images was formed from a precursor solution of 1 M calcium nitrate and 0.6 M phosphoric acid. Scale bars are 300 nm for part a, and 100 nm for part b.

droplet reactors, which is controlled with the flow rates and the geometry of the glass capillary microfluidic devices.[29] Even though only glass microcapillary devices are used in the present study, the concept of using double emulsion droplets as microreactors is also applicable to double emulsions generated by other techniques.[42]

Properties of HAp Powders Processed with Double Emulsions. *Microstructural Analysis Using SEM and TEM*. The powder obtained after washing and drying of the precipitates exhibits unique microstructures with high surface area. After repeated washing of the precipitates with water and then drying at 40 °C, the original spherical aggregates of the precipitates are not retained in the dried powder shown in Figure 4a. At higher magnification, the powder appears to be made up of 1-μm spherical particles that form clusters as shown in Figure 4b. It is most likely these spherical particles that are the precipitates that stick with each other to form the aggregates shown in Figure 3. Small aggregate particles, about 1 μm in diameter, can be seen in the loose aggregate in Figure 3a and also on the edges of the denser aggregates in Figures 3b and c. At higher magnification, each spherical particle appears to assemble from needlelike nanoparticles connected to each other at the center of the sphere, forming a feathery morphology, as shown in Figure 4c. The needlelike nanoparticles can be clearly observed in the TEM images shown in Figure 5. These nanoparticles, which have a length of about 50 nm and a typical aspect ratio of 10 or more, overlap with each other to form a network as shown in Figure 5b. The precise nanostructure of the hydroxyapatite formed likely varies with different reaction conditions, such as pH and temperature, as demonstrated in synthesis techniques using surfactants as template.[27]

BET Surface Area Analysis. The unique morphology of the HAp powders synthesized in the double emulsion droplet reactors gives rise to a high porosity and surface area. For an inner solution with 1 M calcium and 0.6 M phosphorus precursor concentrations, the BET surface

(42) Steinbacher, J. L.; Moy, R. W. Y.; Price, K. E.; Cummings, M. A.; Roychowdhury, C.; Buffy, J. J.; Olbricht, W. L.; Haaf, M.; McQuade, D. T. *J. Am. Chem. Soc.* **2006**, *128*(29), 9442–9447.

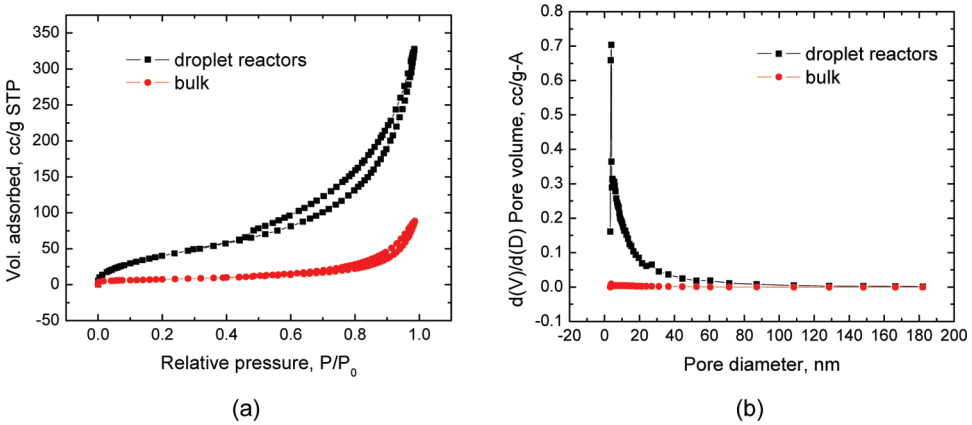

Figure 6. (a) Nitrogen adsorption/desorption isotherms and (b) pore size distributions of hydroxyapatite in double emulsion droplet reactors and in bulk. The powder examined was formed from a precursor solution of 1 M calcium nitrate and 0.6 M phosphoric acid.

area of the powder is 162.8 m^2/g; by comparison, powders obtained from bulk reaction typically have a BET surface area of 26.0 m^2/g. In the absence of any micellar templates or catalysts, our powder achieves a higher surface area than powders prepared with a hydrothermal method (31−43 m^2/g)[17] or a reverse micelle synthesis (52 m^2/g)[20] and a surface area comparable with powders prepared with a catalyzed process (173 m^2/g).[43] The nitrogen sorption isotherms for both powders exhibit hysteresis loops, which are characteristic of mesoporous type IV isotherms, as shown in Figure 6a. However, the volume adsorbed is consistently higher at all relative pressure for the powder prepared in the double emulsion droplet reactors, in agreement with its higher surface area. The total pore volume is 0.499 mL/g for the powder prepared in double-emulsion-droplet reactors, as compared to 0.133 mL/g for the powder prepared in bulk. Apart from having more pore volume, the powder formed in droplets also has a different pore size distribution, as shown in Figure 6b. While both powders have a large proportion of pores with diameters between 20 and 80 nm, the powder prepared in droplets also has about 20% of its pores with diameters under 6 nm. While most previous studies focus on the engineering of pores in the microscale,[11,44−46] our technique offers a novel route to synthesis HAp powders with nanosized pores. Introduction of nanosized pores significantly enhances the total surface area of the powder. It will also promote integration of the powder with other materials for improved mechanical properties. Nanostructuring can also potentially improve the mechanical properties of hydroxyapatite after pressureless sintering[27] while microporosity in the hydroxyapatite can facilitate the adsorption of proteins and further the adhesion and proliferation of human bone cells.[47]

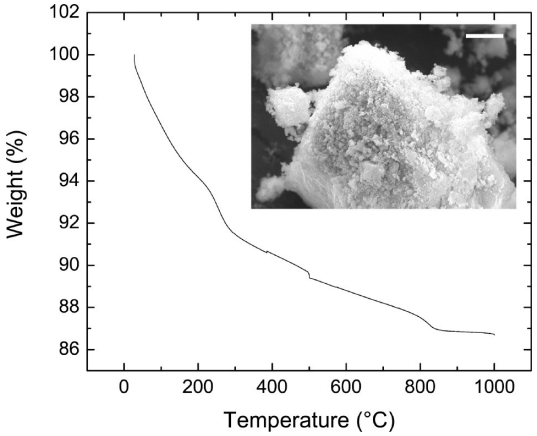

Figure 7. Thermogravimetric (TG) curves of the hydroxyapatite formed. The sample heating rate was 5 °C/min, and the sample was calcined at 500 and 1000 °C each for 10 min. The inset is a scanning electron microscope (SEM) image of the powder after thermogravimetric analysis. The powder examined was formed from a precursor solution of 1 M calcium nitrate and 0.6 M phosphoric acid. Scale bar in the inset is 5 μm.

Biomolecules and drugs can also adsorb onto the powders and interface with each other on the nanometer-sized scale to increase bioactivity.

Phase Analysis. For phase and compositional analysis, the powder is heat-treated or calcined at various temperatures. From thermogravimetric analysis (TGA), the powder formed in the droplet reactors first experiences a steady decrease in weight until about 200 °C due to the evaporation of adsorbed water and other low boiling point contaminants, if any, as shown in Figure 7. At ~250 °C, the weight drops at a higher rate until ~300 °C. The slope of the curve remains almost the same until about 820 °C where another dip occurs. The weight loss until 820 °C is attributed to carbon loss from the system, due to the high heating rate of 5 °C/min. The weight of the sample then starts to level off at about 86.5% above 850 °C. The sudden sharp drop in slope at 500 °C is due to the 10-min holding time at the temperature and does not correspond to any change in phase. To study the phase transformations behavior, room temperature XRD has been used to analyze the powder after calcinations at various temperatures. The XRD patterns for powders

(43) Hoffmann, C.; Zollfrank, C.; Ziegler, G. *J. Mater. Sci.−Mater. Med.* **2008**, *19*(2), 907–915.
(44) Tang, F.; Fudouzi, H.; Uchikoshi, T.; Sakka, Y. *J. Eur. Ceram. Soc.* **2004**, *24*(2), 341–344.
(45) Almirall, A.; Larrecq, G.; Delgado, J. A.; Martinez, S.; Planell, J. A.; Ginebra, M. P. *Biomaterials* **2004**, *25*(17), 3671–3680.
(46) Tsuruga, E.; Takita, H.; Itoh, H.; Wakisaka, Y.; Kuboki, Y. *J Biochem.* **1997**, *121*(2), 317–324.
(47) Myriam, R.; Olivier, G.; Eric, C.; Joseph, D.; Pierre, H.; Karine, A. *J. Biomed. Mater. Res. Part A* **2006**, *78A*(2), 222–235.

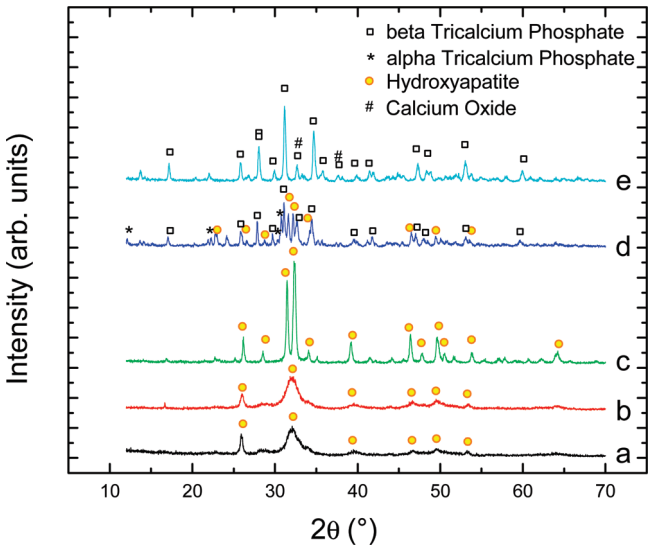

Figure 8. X-ray diffraction (XRD) patterns of hydroxyapatite powder (a) as-formed and calcined at (b) 600, (c) 800, and (d) 1000 °C. Samples were heated at 30 °C/min to the temperature specified and then kept at the same temperature for one hour. (e) XRD pattern of powder heated at 5 °C/min to and calcined at 1000 °C. All powders examined were formed from a precursor solution of 1 M calcium nitrate and 0.6 M phosphoric acid. The squares, stars, circles, and pound signs designated as β-tricalcium phosphate (TCP), α-tricalcium phosphate, hydroxyapatite, and calcium oxide indicate the characteristic peaks of α-TCP (JCPDS no. 09-0348), β-TCP (JCPDS file no. 09-0169), hydroxyapatite (JCPDS file no. 09-0432), and calcium oxide (JCPDS no. 82-1691) at the marked positions, respectively.

before and after calcinations at 600 °C appear very similar to those that show signature peaks for HAp (JCPDS no. 09-0432), as shown in the curves labeled a and b in Figure 8. The peaks are wide indicating that the powder is still partially amorphous even after calcination at 600 °C for 1 h. The peaks obtained from the powder after calcination at 800 °C for 1 h become significantly sharper, revealing pure crystalline HAp phase, as shown in the curve labeled c in Figure 8. Interestingly, after the powder has been calcined at 1000 °C for 1 h, more peaks appeared in the powder XRD pattern, as shown in the curve labeled d in Figure 8. A combination of peaks primarily from both HAp and β-TCP ($Ca_3(PO_4)_2$) (JCPDS no. 09-0169) phases are observed with a small amount of α-TCP (JCPDS no. 09-0348). If the powder is left for calcination at a slower rate of 5 °C/min, instead of 30 °C/min, the powder is completely converted to β-TCP and CaO (JCPDS no. 82-1691), as indicated by the curve labeled e in Figure 8. Similar conversion to β-TCP has also been observed during high temperature sintering of porous HAp in air.[48] In summary, the powder formed in our droplet microreactors is predominantly amorphous calcium phosphate, which can be transformed to crystalline HAp and other phases of calcium phosphates by calcination. The precise composition of the final powder is likely to be influenced by the reaction conditions in the droplet reactors. A better understanding of the influence may ultimately enable manipulation of the compositions of the powder.

(48) Tian, J. T.; Tian, J. M. *J. Mater. Sci.* **2001**, *36*(12), 3061–3066.

Overall, our results offer direct visualization of HAp formation from its precursors in microreactors. With our droplet microreactors, the evolution of the macroscale morphology can be monitored in isolated droplets. Since the shells of the double emulsion droplets have roughly the same thickness, each droplet can be treated as an identical reactor, making it possible to monitor large number of droplets simultaneously. This is difficult to achieve with other methods. Visualization of HAp formation helps us to understand different stages of formation as well as influence of precursor concentration on the morphology of as-formed mesoporous HAp powders. Lower precursor concentration in the microreactor helps form first a highly porous networked nanostructured HAp; then, with time, some consolidation takes place in the as-formed powders within the microreactor (See movie S1 in the Supporting Information). With increasing precursor concentration within the same size of double-emulsion-droplet microreactors, the as-formed HAp morphology changes from an open-ended network mesoporous structure to a dense mesoporous structure. The total pore volume, 0.499 mL/g, is significantly higher for the powder prepared in double emulsion droplet reactors as compared to that prepared in bulk, 0.133 mL/g. While most of the pores are between 20 and 80 nm in diameter for powders synthesized in bulk and in microreactors, the HAp powder prepared in droplet microreactor also has about 20% of pores with diameters under 6 nm. The presence of nanoscale porosity significantly increases the specific average surface area of the as-formed powders to 162.8 m^2/g, as compared to 26.0 m^2/g for powders obtained from bulk reaction. Calcination of as-formed powder up to 800 °C results in the formation of a pure HAp phase.

Conclusions

We present a novel method for synthesizing mesoporous hydroxyapatite (HAp) powders using double emulsion droplets as microreactors. Double emulsion droplets are ideal microreactors as they afford excellent encapsulation of the starting reactants and allow on-demand addition of additional reactants. Our results suggest that the calcium and phosphorus precursors are well encapsulated inside the inner drops of the double emulsion reactors while alkali introduced in the continuous phase effectively adjusts the pH and triggers the CaP formation in the inner drops. The porosity of the HAp aggregates synthesized can be tuned by adjusting the reactant concentration in the inner drop. Aggregate networks of different degrees of compactness have been synthesized by varying the concentrations of the calcium precursor from 0.1 to 1 M, and the phosphorus precursor from 0.06 to 0.6 M. Powder formed with our technique demonstrates remarkable microstructures and significant increase in the total surface area and porosity. The surface area and the total pore volume of the powders prepared are as high as 162.8 m^2/g and 0.499 mL/g, respectively. From our thermal and phase analyses, we confirm that the amorphous CaPs formed is first transformed to crystalline HAp and then at a higher

temperature to β-TCP. Our technique represents a novel way of using double emulsion droplets as microreactors for the synthesis of inorganic particles as well as imaging of the synthesis process. It would also be advantageous to monitor other aspects, such as the chemical compositions and microstructures, during the formation of the hydroxyapatite. If this can be done, we believe these droplet microreactors will lead to a comprehesive understanding of the formation mechanism. The novel synthesis approach will not only improve the performance of calcium phosphate-based materials, but will also enable the control of nanoscale porosity and morphology of other inorganic particles.

Acknowledgment. This work was supported by the NSF (DMR-0602684) and the Harvard MRSEC (DMR-0820484). H.C.S. and D.A.W. were supported in part by BASF Ludwigshafen in Germany. We thank Dr. Christian Holtze for helpful discussions, the Particle Characterization Laboratory of Beckman Coulter, Inc. for the BET measurements, and Dr. William J. Croft for training on the X-ray diffractometer as well as Dr. Hunter Lauten and Prof. David Edwards for the use and help with the TGA experiments.

Note Added after ASAP Publication. There was an error in ref 18 in the version published ASAP October 16, 2009; the corrected version was published ASAP October 20, 2009.

Supporting Information Available: Movie showing the evolution of the droplet reactor during formation of hydroxyapatite. This material is available free of charge via the Internet at http://pubs.acs.org.